Int. J. Electrochem. Sci., 8 **(2013)** 12078 - 12087

International Journal of
ELECTROCHEMICAL
SCIENCE
www.electrochemsci.org

Application of Tin Sulfide-Tin Dioxide Nanocomposite as Oxygen Gas-Sensing Agent

Hassan Karami[1,2,*], *Somayyeh Babaei*[1]

[1]Nano Research Laboratory, Department of Chemistry, Payame Noor University, Abhar, Iran
[2]Department of Chemistry, Payame Noor University, 19395-4697, Tehran, I.R. of Iran
[*]E-mail: karami_h@yahoo.com

Received: 2 July 2013 / *Accepted:* 29 August 2013 / *Published:* 25 September 2013

Tin sulfide-tin dioxide nanocomposite is synthesized by the pulsed-current electrochemical method on the surface of tin substrate. The prepared sample in conditions includes 92 $mA.cm^{-2}$ current density, 13 Hz pulse frequency, 0.008 M sodium sulfide, pH 12.5, and 25 °C electrocrystallization temperature is characterized by scanning electron microscopy (SEM), transmission electron microscopy (TEM), and X-ray diffraction (XRD) techniques. Characterization studies showed that the sample contains uniform SnS-SnO2 nanocomposite in orthothombic nanorod form with 30 nm average diameters and 200 nm average lengths is synthesized. The synthesized is used as an oxygen gas-sensing agent to construct a new solid-state sensor. This sensor showed high dynamic range, high sensitivity to oxygen gas, fast response time and very low memory effect without any interference of the other gases.

Keywords: tin sulfide-tin dioxide nanocomposite; pulsed current; electrochemical synthesis; oxygen; gas sensor

1. INTRODUCTION

Nanostructured materials have attracted much attention in various fields of science and technology [1-2]. A variety of physicochemical methods, including metal evaporation [3], spray pyyrolysis [4], sol-gel [5] and electrochemical methods [6] have been used to produce nanometer-sized materials.

Band gaps of tin sulfide and tin dioxide as IV-VI group semiconductors are 1.48 (or smaller) and 4.08 eV (or smaller), respectively. The properties of these materials can change by any variation in morphology or particle sizes. Different morphologies include nanoparticles [7-10], nanostructures [11], nanoholes [12], nanorods [13], nanoplanes [14], nanowires [15-17], nanodiscs [18-20], and

orthorhombic structures [21]. All of these morphologies can be prepared by different methods, such as hydrothermal [22], vapor condensation [23-28], electrochemical precipitation [29-31], chemical methods [32], and spray and hot plate pyyrolysis [33]. Tin sulfide and tin dioxide nanoparticles have wide applications in many fields such semiconductors, photovoltaic materials, solar cells, lithium ion batteries, photocatalysts, and also as gas- sensing agents in the solid- state sensors [34-36].

There are not many reports about using SnS, SnO_2 and their composites as a gas-sensing agent. Porous flower-like tin oxide (SnO_2) nanostructure were synthesized by Huang et al. by annealing of the flower-like tin sulfur (SnS_2) nanostructures [37]. These nanostructures exhibit a good response and reversibility to some organic gases, such as ethanol, to methanol, 2- propanol, acetone and *n*-butanol.

Mixed SnO_2 nanoparticles with 1 %wt MWCNTs used as NO_2, NH_3, and xylene gas sensors by Park et al [38]. The fabricated gas sensors were characterized to NO_2, NH_3, and xylene gases, respectively, as a function of concentration at 300 ºC and temperature from 180 ºC to 380 ºC at constant concentration. Authors noted that the fabricated micro-gas sensors could be used for ubiquitous sensor network applications to monitor environmental pollutants in the air with good sensitivity and selectivity at low power operation below 30 mW.

SnS nanoparticles were prepared through directly dispersing melted tin in a sulfur-dissolved solvent by Zhang et al [39]. The as-prepared SnS nanoparticles display novel blue-UV emission, promising for applications in optical devices.

Comini et al developed a gas sensor based on tin oxide nanobelts with a simple DC-resistive measurement in 2002 [40]. A platinum interdigitated electrode was made using sputtering technique with shadow masking on alumina substrate. Then, a bunch of nanobelts was transferred onto the electrodes for electric conductance measurements, the gases tested were CO, NO_2 and ethanol that are important for environmental applications, for breath analyser and food quality control. CO and ethanol were found to increase the conductivity that is common for an *n*-type semiconductor such as tin oxide.

In another work, SnO_2 Nanobelts and nanowires were mixed with CuO and used as H_2S gas sensing agent [41]. The increase in H_2S response was confirmed in 1D nanostructure, the detection limit reached was lower than 3 ppm. Of course the addition of a polycrystalline material reduces the advantages of the use of single crystalline metal oxide as sensing layer.

Yu et al recently published a contribution on tin oxide nanobelts proving their integration with micro-machined substrate [42] which is crucial if a real application is envisaged, and showing their sensitivity to nerve agent, an application of increasing interest for security reasons.

Maffeïs et al used nano-crystalline SnO_2 to detect the O_2 and CH_4 gases at elevated temperatures [43].

Jiménez et al investigated the gas sensing ability of SnO_2 powder as O_2/H_2 gases sensing agent. They found that the texture and previous treatments are the critical factors determining the gas sensing properties of SnO_2 and Pd/SnO_2 samples [44].

In this work, we use pulsed-galvanostatic method to synthesize tin sulfide-tin dioxide nanocomposites. The synthesized SnS-SnO_2 nanocomposite sample was used to construct a solid- state sensor to detect oxygen gas.

2. EXPERIMENTAL

2.1. Materials

Copper (II) sulfate ($CuSO_4$) and acetone were purchased from Merck and were used without any purification.Sodium sulfide (Na_2S) was obtained from Loba Chimie Co. (India). Sodium dodecyl sulfate (SDS), polyvinyl pyrrolidone (PVP), glycerol, and cetyltrimethyl ammonium bromide (CTAB) were purchased from Fluka and Aldrich. Pure tin substrate was prepared from the national iranian Simaran company. Double-distilled water was used in all experiments.

2.2. Instrumental

MPS-3010L model of a power source, made by the Taiwan Matrix company was used for making a constant current. A home-made electrical pulse apparatus was applied to make the reproducible current pulses. The temperature of the synthesis solution was controlled by circulator (HAKKEL model), made by Fisons company (Germany).

The synthesized SnS-SnO_2 nanocomposite was characterized by the scanning electron microscopy (SEM, Philips, XL-30, and The Netherlands), transmission electron microscope (TEM, Zeiss EM900, 80 keV) and X-ray powder diffraction (Philips X'pert diffractometer using Cu [(Kα)] radiation with λ= 0.15418 nm).

2.3. Procedures

2.3.1. Synthesis procedure

Before each electrochemical deposition, the metal tin electrodes were placed in the 35 %wt HNO3 for 30 s and then rinsed with double-distillated water to remove any surface oxidized species in contact with air. Two stainless steel cathodes coupled with the prepared tin electrode as anode of the electrochemical cell. The electrodes were put in the synthesis solution including 0.008 M Na_2S, and temperature of 25 °C. The pH of synthesis solution was adjusted at 12.5 by adding NaOH solution. By applying current pulse, SnS-SnO_2 nanoocomposites were directly synthesized on the surface of tin electrode (anode) by oxidation of the tin substrate. The morphology and particles sizes of the samples were characterized by SEM and TEM. XRD patterns (using Cu [(Kα)] radiation with λ = 0.15418 nm) were used to determine the composition of the samples.

2.3.2. Construction of gas- sensing device

A polyacrylamid plate (1 mm × 50 mm × 70 mm) was used as a base material of sensor device (microchip). Two copper comb electrodes were deposited on one side of the plate by the copper electroless process. The surface of copper electrodes was covered by gold electroplating. Figure 1 shows the scheme of gas sensing device.

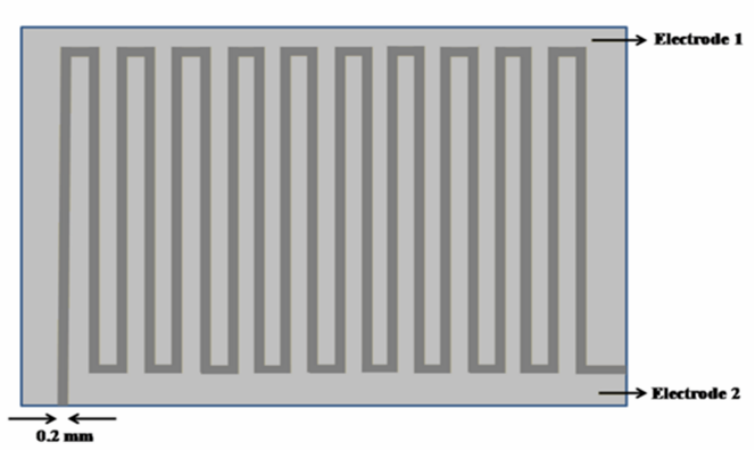

Figure 1. Scheme of the constructed sensor microchip (gas sensing device).

We dispersed 0.2 g optimized SnS-SnO_2 nanocomposite in 5 ml acetone by ultrasonic shaking for 2 h to obtain a homogenous suspension (slurry). The surface of microchip was fully covered by the homogenized slurry. The microchip was kept in 100 °C for 10 min to evaporate the solvent to form a nanostructured thin film on the surface of the microchip. The coated microchip was cured at different temperatures (110, 120 and 130 °C) for 2 h to determine a suitable cohesion temperature of the SnS-SnO2 nanocomposites, enabling them to adhere to one another and to the microchip surface.

The cured microchip was input into a glassy cubic box of 32 L total volume. A small electric fan was used to make fast homogenization of the gas mixture in the box. The different volumes of some gases, such as NH3, O_2, H_2O, CO, H_2, and LPG (Town gas) were injected into the box, and the sensor resistance was measured.

The final gas concentration ($C_{(ppm)}$) was calculated based on the following equation (Eq. 1):

(Eq. 1) $$C_{(ppm)} = \frac{V_{Injected}}{V_{Box}} \times 10^6 = \frac{V_{Injected}}{3.2 \times 10^4} \times 10^6 = 31.25 \times V_{Injected}$$

Where, the box volume is 32 L (3.2×10^4 ml) and other volumes are also in ml.

3. RESULTS AND DISCUSSION

3.1. Sample characterization

The synthesized sample was characterized by SEM, TEM and XRD methods. In Fig. 2, the morphology and particles sizes of the synthesized sample are shown by SEM and TEM images.

Based on Fig. 2, the sample consists nanorods with 30 nm average diameters and 200 nm average lengths. Figure 3 shows the XRD patterns of these samples. Based on XRD patterns, the synthesized sample include 63 %wt tin sulfide and 37 %wt tin dioxide.

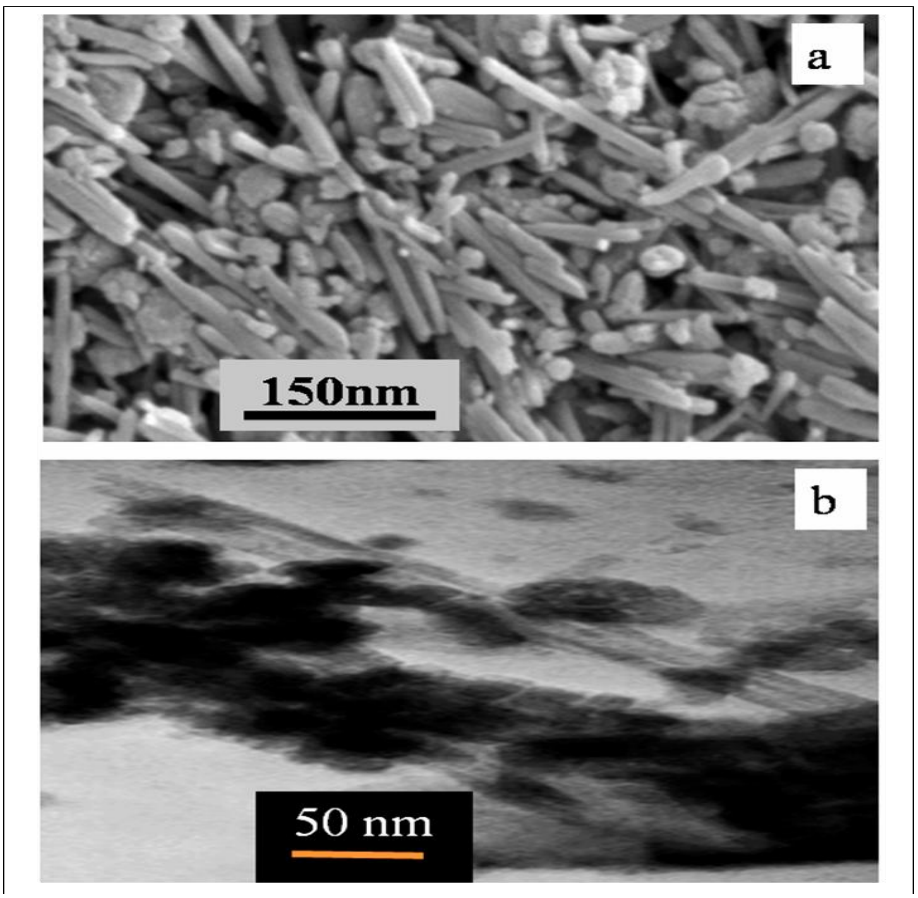

Figure 2. SEM image with 30000 magnification (a) and TEM image with 60000 magnification (b) of the optimized SnS nanorods.

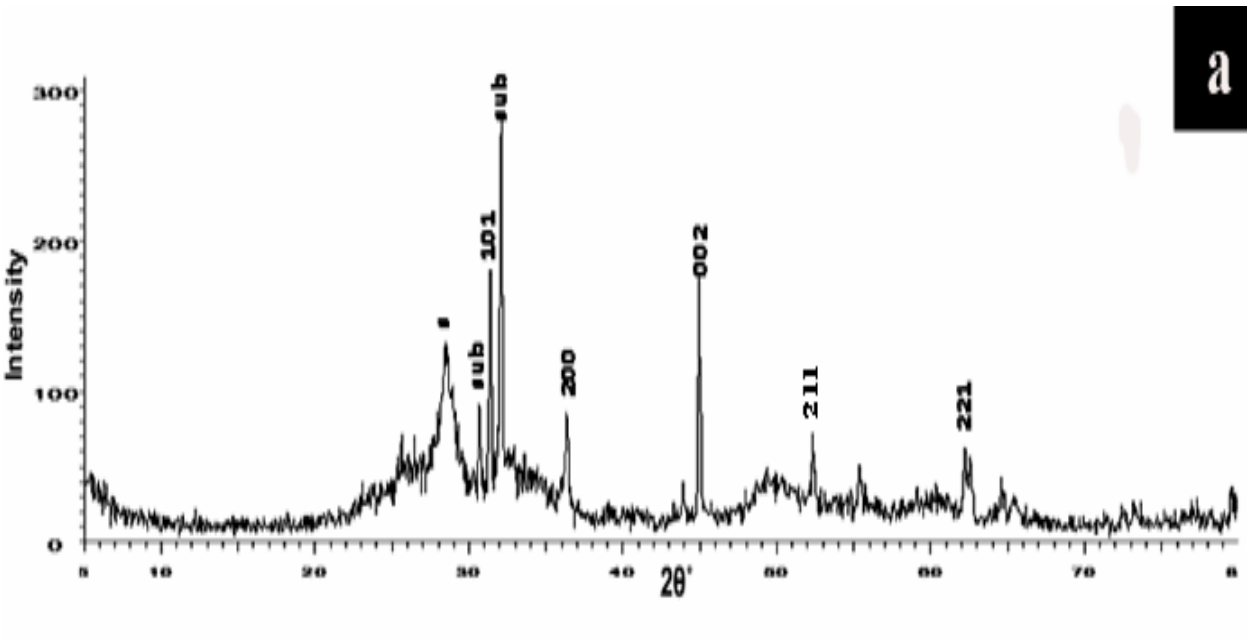

Figure 3. XRD patterns of the synthesized SnS-SnO_2 nanocomposite.

3.2. Application of SnS nanorods as a gas sensor

After optimization of the synthesis conditions, the optimized SnS-SnO_2 nanocomposite was used as a gas-sensing agent. As mentioned in the experimental sections, the preparation steps were exactly performed. The effects of different gases like H_2O, NH3, O_2, CO, H_2, and Town gas were investigated on the Ohmic resistance of the prepared microchip (Fig. 4). As we can see in Fig. 4, a variation in the concentration of NH3, H_2O, CO, H_2, and Town gases has no acceptable effects on the sensor's electrical resistance. Consequently, this sensor is unsuitable for measuring these gases. But about O_2, the sensor shows good responsibility.

About gas sensing mechanism, it is obvious that the sensing gas should be adsorbed on the surface of sensing agent (SnS-Sno_2 nanocomposite) to change its electrical conductivity. When the sensor doesn't show a acceptable responses for NH3, H_2O, CO, H_2, and Town gases, it shows that these molecules cannot adsorb on the surface of gas sensing agent or cannot change its conductivity.

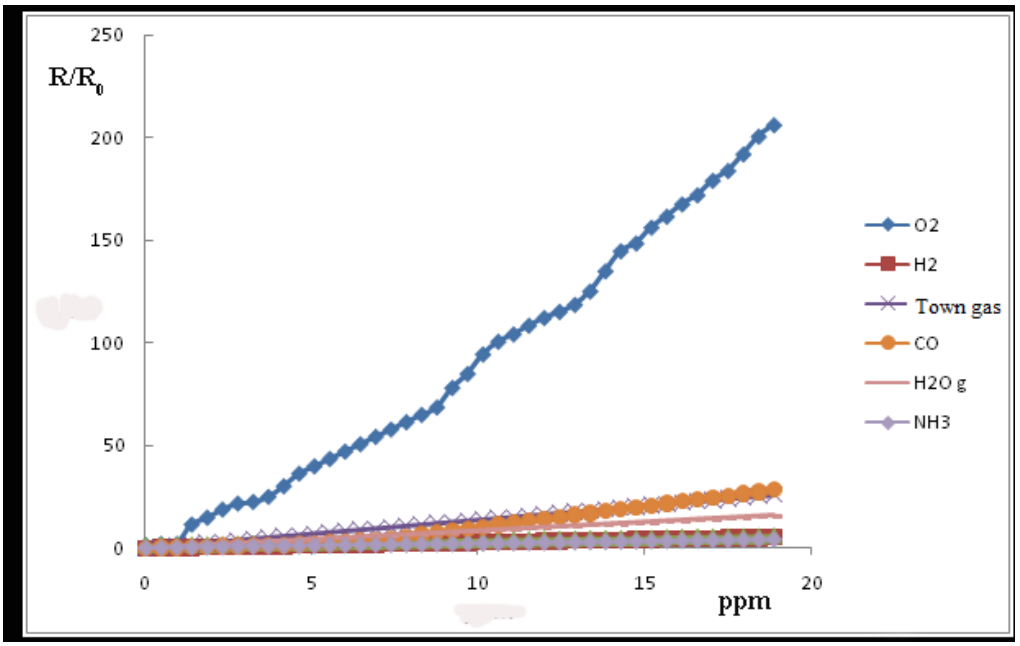

Figure 4. The sensor response for different concentrations of various gases at temperature of 128 ºC.

The effect of variations in O_2 concentration was investigated on the sensor resistance at 25, 75, and 128 °C and the linear rage of the obtained results were represented in Fig. 5. It is obvious in Fig. 5, by increasing the measuring temperature, the sensor ability is increased.

For more clarifications, the linear ranges of the sensor response versus oxygen concentration were shown in Fig. 6. As we see in this figure, by increasing the measuring temperature, the linear range and the response sensitivity (the slope of calibration curve) are improved. It should be mentioned, at higher temperature the substrate of microchip shrink. At temperature of 128 °C, the curve shows a maximum slope and consequently, the most sensitivity to oxygen. The calibration equations were calculated as (y = 0.025 x + 1.042), (y = 4.866 x -7.367), and (y =11.46 x- 20.23) for

O_2 at 25, 75 and 128 °C respectively. As we see in these Figures, the response sensitivity (calibration slope) of the sensor is maximum (11.46 Ω ppm^{-1}) at 128 °C. Therefore, oxygen gas can be determined by the manufactured sensor exactly at optimum temperature of 128 °C without any interference of the other gases.

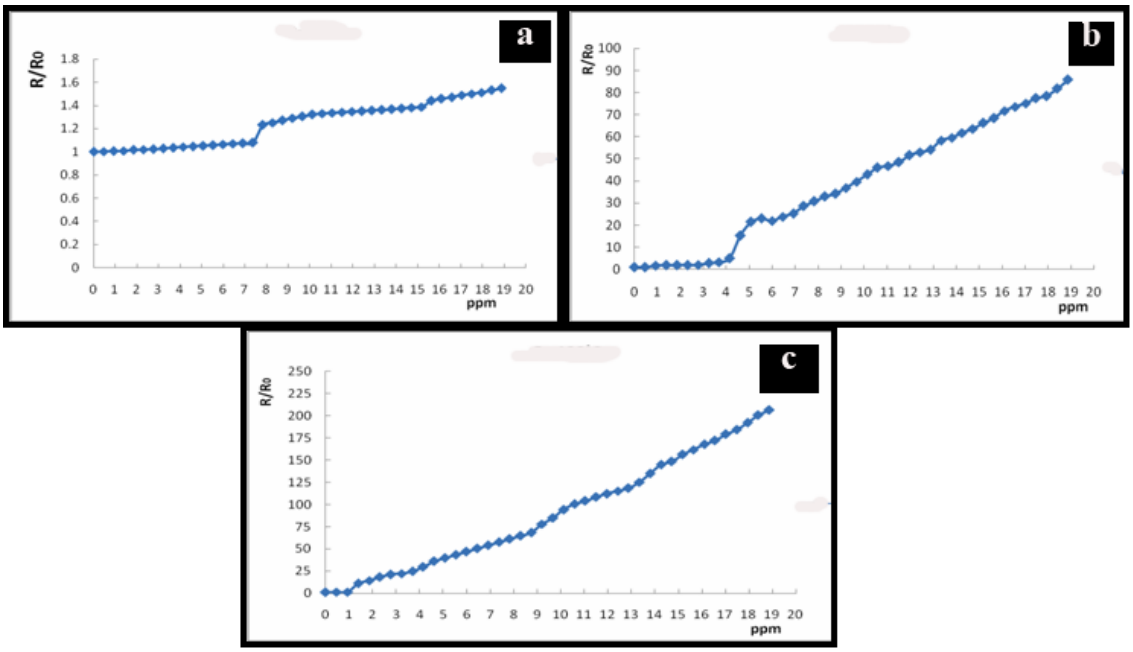

Figure 5. The sensor response for different concentrations of O_2 at temperatures of 25 ºC (a) 75 ºC (b) and 128 ºC (c).

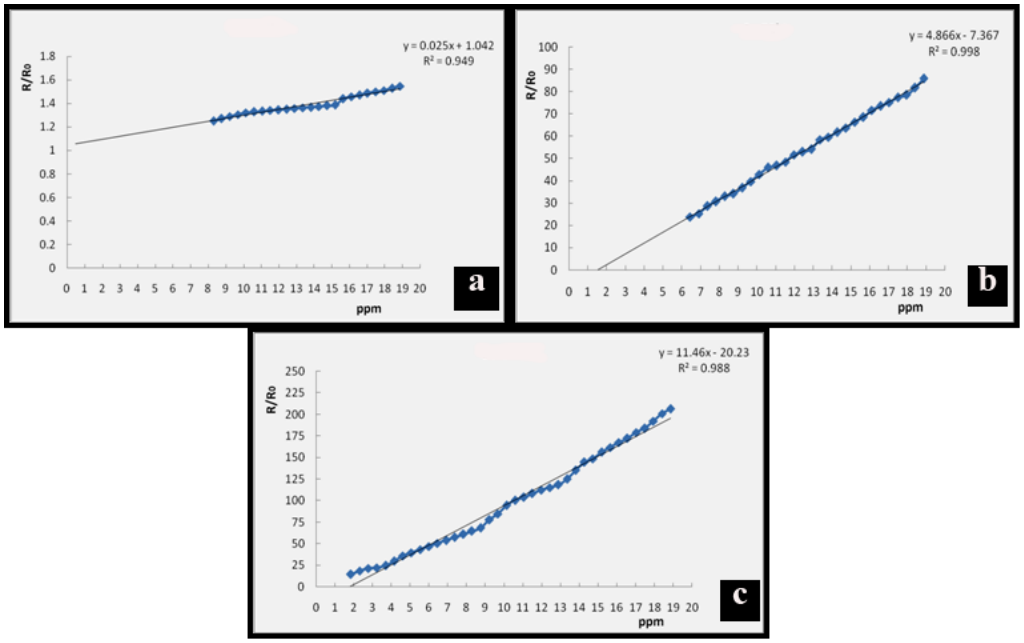

Figure 6. Calibration curves for measurement of O_2 at temperatures of 25 ºC (a) 75 ºC (b) and 128 ºC (c).

3.9. Sensor ability for the measurement of O_2

The modified sensor was applied to measure the concentration of O_2 in an artificial medium with 24 ppm CO, 24 ppm Town gas, and 7 ppm O_2 in presence of N_2. The results are presented in Table 1. In every step, the concentration of O_2 in the box was determined by plotting calibration curves with 6, 8, 10, and 12 ppm O_2 standard gas mixture. The used calibration curve was shown in Fig. 7. The precision of the results was confirmed by T-test. The value of t_{n-1} with a confidence level of 95% is equal to 4.30. The experimental *t* (2.12) is less than 4.30; consequently the average value of three measurements (7.09 ppm) doesn't have any significant difference from the real value (7 ppm). Also, detection limit and reproducibility of the method was calculated 1% as RSD and 0.9 ppm respectively, that provides high precision of it. The obtained results showed the presented sensor has some advantages such as low RSD, low detection limit and high sensitivity with respect to the previous reports about solid state sensors for O_2 gas [45-48].

Table 1. Results of sensor application for measurement of O_2 in presence of CO, N_2 and Town gas

Experiment number	Initial concentration (ppm)	Resulted concentration (ppm)
1	7	7.36
2	7	7.05
3	7	6.85

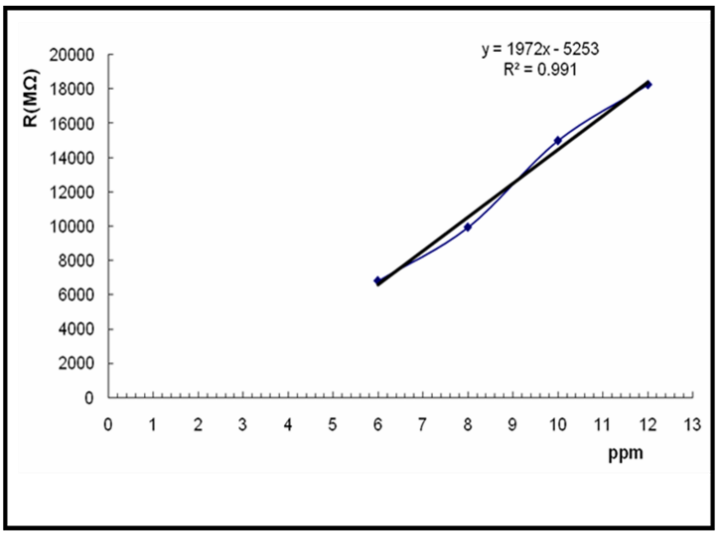

Figure 7. Calibration curve for measurement of O_2 in concentrations of 6, 8, 10 and 12 ppm.

3.9. Sensor response time

To obtain response time, we determined the changes in relative sensor resistance versus the time. Based on the obtained results, the average amounts for adsorption and desorption process of

oxygen gas on the sensing material were 52 s and 38 s, respectively. Fast adsorption and desorption is a main advantages of a gas sensor. For the constructed sensor, desorption time of O_2 is lower that's adsorption. It is an important advantage which causes to decrease the memory effects of the proposed sensor.

4. CONCLUSIONS

Tin sulfide/tin dioxide nanocomposites can be synthesized by pulsed- current electrochemical method from a basic sodium sulfide solution. The synthesized SnS-SnO_2 nanorods act as successive and sensitive agent in the solid- state sensor to measure oxygen concentration in the gas mixtures.

ACKNOWLEDGEMENTS
We gratefully acknowledge the support of this work by Abhar Payame Noor University Research Council.

References

1. E. Manova, T. Tsoncheva, D. Paneva, I. Mitov, K. Tenchev, L. Petrov, *Appl. Catal. A: Gen* 277 (2004) 119-127.
2. Mao-Sung Wu, Pin-Chi J. Chiang, Jyh-Tsung Lee, Jung-Cheng Lin, *J. Phys. Chem*. B 109 (2005) 23279–23284.
3. L. Carbone, S. Kudera, E. Carlino, W. J. Parak, C. Giannini, R. Cingolani, L. Manna, *J. Am. Chem. Soc.* 128 (2006) 748-755.
4. M. Regragui, M. Addou, A. Outzourhit, J. C. Bernede, E. E. Idrissi, E. Benseddik, A. Kachiuane, *Thin Solid Films* 358 (2000) 40-45.
5. J. Xie, X. Cao, J. Li, H. Zhan, Y. Xia, Y. Zhou, *Ultrason. Sonochem*. 12 (2005) 289-293.
6. Kh. Ghanbari, M. F. Mousavi, M. Shamsipur, *Electrochim. Acta* 52 (2006) 1514-1522.
7. S. Y. Hong, R. Povitz, Y. Prior, R. Tenne, *J. Am. Chem. Soc*. 125 (2003) 10470-10476.
8. A. L. Rogach, A. Eychmuller, S. G. Hickey, S. V. Kershaw, *Small* 3 (2007) 536-739.
9. J. M. Luther, M. C. Beard, Q. Song, M. Law, R. J. Ellingson, A. Nozik, *J. Nano. Lett*. 7 (2007) 1779-1784.
10. D. V. Talapin, C. B. Murray, *Science* 310 (2005) 86-91.
11. N. Petkov, J. Xu, M. A. Morris, J. D. Holmes, *J. Phys. Chem*. C 112 (2008) 7345-7349.
12. K. Jiang, Y. Wang, J. Dong, L. Gui, Y.Tang, *Langmuir* 17(2001) 3635-3639.
13. T. Kim, D. Son, M. Choi, B. Parc, *J. Power Sources* 167 (2007) 529-533.
14. J. Seo, J. Jang, S. Park, C. Kim, B. Park, *J. Chon, Adv. Mater* 20 (2008) 4269-4275.
15. S. K. Panda, A. Datta, A. Dev, S. Gorai, S. Chaudhuri, *Crystal Growth* 6 (2006) 2177-2182.
16. S. Vaucher, M. Li, S. Mann, *Angew. Int. Ed*. 39 (2000) 1793-1799.
17. Z. Y. Zhong, Y. D. Yin, B. Gates, Y. N. Xia, *Adv. Mater*. 12 (2000) 206-211.
18. S. Boonsalee, R. W. Gudavarthy, J. A. Bohannan, *Chem. Mater*. 20 (2008) 5737-5742.
19. S. Cheng, G. Chen, Y. Chen, C. Huang, *Opt. Mater*. 29 (2006) 439-444.
20. L. R. Bohannan, E. W. Switzer, G. A. Oba, *Appl. Phys. Letters* 83 (2003) 1944-1952.
21. J. Kang, J. Park, D. Kim, *Electrochem. Commun*. 12 (2010) 307-310.
22. H. Hu, B. Yang, J. Zeng, Y. Qing, *Mat. Phys*. 86 (2008) 233-239.
23. L. S. Price, I. P. Parking, A. M. E. Hardy, R. Clark, *Chem. Mater*. 11 (1999) 1792-1799.

24. T. Jiang, G. A. Ozin, *J. Mat. Chem*. 8 (1998) 1099-1108.
25. B. Polosz, W. Steurer, H. Schulz, *Acta Crystallogr. Sect*. B 46 (1990) 449-455.
26. A. Ortiza, J. C. Alonso, M. Garcia, J. Toriz, *Semicond. Sci. Technol*. 11 (1996) 243-249.
27. I. P. Parking, A. T. Rowley, *Polyhedron* 12 (1993) 2961-2968.
28. A. Ortiz, S. Lopez, *Semicond. Sci. Technol*. 9 (1994) 2130-2136.
29. P. Bilijana, G. Lavan, T. Atanas, *Chem. Phys*. 83 (2004) 245-249.
30. M. M. Elnahass, H. M. Zeyada, *Opt. Mater*. 20 (2002) 159-165.
31. L. Sato, M. Ichimura, E. Aria, Y. Yamazaki, *Sol. Eng. Mater. Sol. Cell* 85 (2005) 153-157.
32. Y. Liu, D. Hou, G. Wang, *Chem. Phys. Lett*. 379 (2003) 67-72.
33. G. H. Yue, D. L. Peng, P. X. Yan, *J. Alloy. Compd*. 468 (2009) 254-258.
34. Y. Wang, H. Gong, B. Fan, G. Hu, *J. Phys*. C 114 (2010) 3256-3264.
35. D. Giri, K. K. Das, *J. Phys*. A 109 (2005) 7207-7212.
36. B. J. Seo, J. Jang, S. Park, C. Kim, B. Park, *Adv. Mater*. 20 (2008) 4269-4275.
37. J. Huang, K. Yu, C. Gu, M. Zhai, Y. Wu, M. Yang, J. Liu, *Sens. Actuators* B 147 (2010) 467-474.
38. K. Choi, J. Park, K. Park, H. Kim, H. Park, S. Kim, *Sens. Actuators* B 150 (2010) 65-72.
39. Y. Zhao, Z. Zhang, H. Dang, W. Liu, *Mater. Sci. Eng*. B 113 (2004) 175-178.
40. E. Comini, G. Faglia, G. Sberveglieri, Z. Pan, Z.L. Wang, *Appl. Phys. Lett*. 81 (2002) 1869-1871.
41. X. Kong, Y. Li, *Sens. Actuators* B 105 (2005) 449-453.
42. E. Comini, *Analytica Chimica Acta* 568 (2006) 28-40.
43. T. G. G. Maffeïs, G. T. Owen, M. W. Penny, T. K. H Starke, S. A. Clark, H. Ferkel, S. P. Wilks, *Surf. Sci.* 520 (2002) 29-34.
44. V.M. Jiménez, J. P. Espinós, A. R. González-Elipe, *Sens. Actuators B* 61 (1999) 23-32.
45. N. Izu, N. Oh-hori, M. Itou, W. Shin, I. Matsubara, N. Murayama. *Sens. Actuators B* 108 (2005) 238-243.
46. J. C.Belmonte, J. Manzano, J. Arbiol, A. Cirera, J. Puigcorbé, A. Vilà, N. Sabaté, I. Gràcia, C. Cané, J. R. Morante, *Sens. Actuators B* 114 (2006) 881-892.
47. Y. Hu, O. K. Tan, W. Cao, W. Zhu, *Ceram. Int.* 30 (2004) 1819-1822.
48. N. Izu, W. Shin, N. Murayama, *Sens. Actuators B* 93 (2003) 449-453.